JOURNAL OF MATERIALS SCIENCE 21 (1986) 4257–4261

A STEM study of grain-boundary segregation in Al–6.5 wt% Mg alloy

D. C. PAINE, G. C. WEATHERLY, K. T. AUST
Department of Metallurgy and Materials Science, University of Toronto, Toronto, Canada

A STEM-EDX analysis study of grain-boundary segregation in an Al–6.5 wt% Mg alloy is presented. STEM-EDX analysis using an electron probe size of 1 nm is shown to provide statistically significant compositional data on grain-boundary segregation in Al–Mg alloys. Solute profiles taken normal to grain boundaries show both non-equilibrium segregation and precipitation phenomena in Al–6.5 wt% Mg alloys water-quenched from 350, 400 and 570° C.

1. Introduction

Considerable controversy exists in the literature about the segregation behaviour of Al–Mg alloys, both in the as-quenched and in the quenched and aged conditions. Indirect evidence of grain-boundary segregation in Al–Mg is based mainly on its grain-boundary corrosion behaviour [1]. This indirect evidence, however, is not supported by all the direct analysis data available in the literature.

Both EDX (energy-dispersive X-ray analysis) and EELS (electron energy loss spectroscopy) have been used previously to attempt to observe directly the segregation of magnesium to grain-boundaries in Al–Mg systems. The results, however, when considering Al–Mg in the as-quenched condition vary even between similar microanalysis techniques. For example, enrichment was seen both by EELS [2] and by EDX [3] while depletion in the as-quenched state has been seen by EELS [4]. More recently [5], TEM/STEM-EDX analysis showed magnesium enrichment at many (but not all) of the as-quenched boundaries observed.

With the exception of Cundy *et al.* [4], all of the above workers considered only the as-quenched state from one temperature (usually around 350° C). In addition, the EDX analysis mentioned above was limited by relatively poor resolution. The dedicated STEM used in the present work to study magnesium segregation in aluminium provides a superior microanalysis resolution, since a smaller electron probe is available.

2. Experimental procedure

An Al–6.5 wt % Mg allow was made with 99.999% Al and 99.99% Mg. The alloy was produced by first induction-melting the components and then bottom-casting into a water-chilled graphite mould. The water cooling was designed to minimize macroscopic segregation due to solute rejection on freezing. The entire casting assembly was contained in a quartz tube which was evacuated and repeatedly backfilled with purified argon. The cast Al–6.5 wt % Mg alloy was rolled to 0.5 mm thick sheet and solution-treated in air for 1 h at 350° C. Without allowing the alloy to cool from 350° C, the Al–Mg sheets were then heated at 400° C for 0.5 h and 570° C for 10 min, followed by water-quenching from each temperature. In addition, some Al–Mg sheets were quenched from 350° C after 1 h. Short annealing times at high temperatures were chosen such that there was sufficient time to allow an equilibrium concentration of vacancies to form but, also, insufficient time for excessive grain growth to occur.

Thin foils for electron microscopy were prepared using a standard dual-jet electropolishing technique. The Al–Mg alloy was thinned using an electropolishing solution consisting of 100 ml perchloric acid and 900 ml ethanol at − 10° C with 15 V applied. All foils were first observed in a TEM, then examined using a Vacuum Generator HB5 dedicated STEM at 100 kV. Extensive use was made of the EDX capability of this instrument. An electron probe size, before beam broadening, of 1 nm was achieved using a 100 μm virtual objective aperture and a 5.8 mrad collection angle. Grain boundaries selected for analysis were oriented parallel, or as close to parallel as possible, to the incident electron beam. On occasions when very long count times were used, specimen drift, if any, was compensated for by stopping the analysis at regular intervals.

2.1. EDX considerations

Using the Tixier and Philibert [6] thin-film criteria, a maximum allowable Al–Mg thin-foil thickness of 300 nm was calculated before absorption corrections became significant, i.e. the absorption of characteristic magnesium X-rays in the aluminium matrix was insignificant for typical foils used in this work (thickness < 200 nm).

However, in the Al–Mg system, the absorption of magnesium characteristic X-rays by carbon contamination may be significant. Many of the Al–Mg foils studied showed carbon contamination. This, combined with beam broadening effects and uncertain ionization cross-sections, would make the quantification of the results difficult. Instead, the ratio of magnesium intensity to the aluminium intensity was plotted.

0022–2461/86 $03.00 + .12

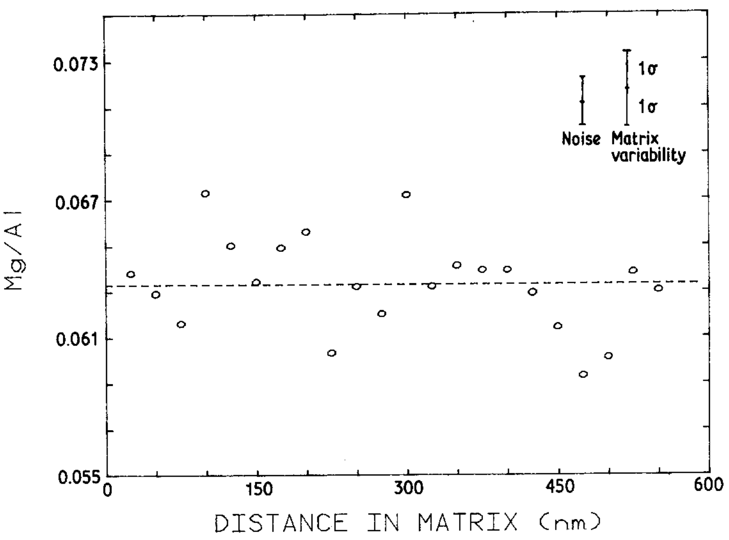

Figure 1 EDX concentration analysis across an apparently defect-free region of the matrix in an Al–6.5 wt % Mg alloy quenched from 570° C.

2.2. STEM analysis procedure

STEM-EDX was used in the analysis of the Al–6.5 wt % Mg alloy. Initially, eleven boundaries were tested to establish whether or not the STEM-EDX system could detect segregation to grain boundaries. The procedure involved grain-boundary analysis in four positions for 50 sec each for a total of 200 sec. This was then compared to a similar analysis of the matrix with four positions, two on either side of the boundary, and chosen approximately 50 nm from the boundary.

When the grain-boundary point analysis was complete, grain-boundary segregation profiles perpendicular to the boundary were produced. This involved analysing for composition in 50 nm intervals away from the boundary over a distance of 300 to 400 nm on either side of the boundary. A count time for the profile analysis of either 100 or 200 sec with a 1 nm probe was used.

An analysis of the error associated with the profile measurements was performed by taking a profile inside an apparently defect-free zone in the matrix. This produced Fig. 1. In order to distinguish between instrument noise and variability as a function of position, pairs of points as close together as possible were analysed every 50 nm over a 600 nm distance. The standard deviation of the peak area difference for adjacent points gives a measure of instrument noise. The total error, which includes sample composition variability and the instrument noise, is simply the standard deviation of all the points. The compositional variance can then be calculated by subtracting the instrument noise variance from the total variance. The square root of the compositional variance is the compositional error.

This procedure for calculating instrument noise makes three assumptions:

1. Concentration does not vary over very short distances.
2. Measurement noise is independent of position for closely spaced points.
3. Measurement noise is also independent of position for large separations of points, to enable the use of widely separated pairs of points.

3. Results

The Al–6.5 wt % Mg alloy was first solution-treated for 1 h at 350° C, then quenched into water. It was subsequently analysed in the STEM after, at most, a 12 h delay between the quench and the STEM observation of the boundary. The analysis procedure first involved analysing in the matrix and again in the boundary (as described earlier) for 200 sec each. It was found that 8 out of 11 boundaries showed significant depletion of magnesium on the boundary. These results are summarized in Table I.

Having established the ability of the STEM to detect segregation or depletion by EDX analysis, a grain-boundary profile of the alloy in the as-quenched from 350° C state was produced. This is shown in Fig. 2. This curve shows only a small depletion; however, the error bars shows that it is significant compared to the bulk variability.

Quenching from 400° C produced significant enrichment, as seen in Figs 3 and 4. Fig. 3 shows the boundary profile of an alloy that had been allowed to age for 18 h at room temperature after the quench. This profile is similar to that shown in Fig. 4, which shows a boundary in an alloy that was stored in liquid nitrogen to prevent ageing.

Finally, Al–6.5 wt % Mg samples were solution-treated at 350° C, then heated to 570° C for 10 min

TABLE I Point analysis of grain boundaries and adjacent matrix region in an Al–6.5 wt % Mg alloy water-quenched from 350° C

Mg/Al ratio		Enrichment (%)
Grain boundary	Matrix	
0.0869	0.0813	6.89
0.0774	0.0794	−2.52
0.0815	0.0830	−1.81
0.0720	0.0881	−18.28
0.0757	0.0707	7.07
0.0733	0.0797	−8.03
0.0816	0.0877	−6.93
0.0769	0.0844	−8.89
0.0679	0.0851	−20.21
0.0837	0.0795	5.28
0.0750	0.0959	−21.79

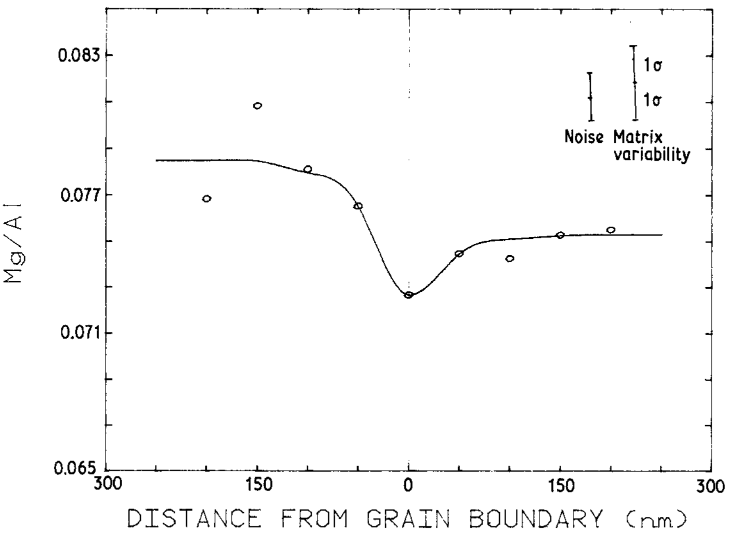

Figure 2 EDX analysis showing the solute concentration profile of a grain boundary in an Al–6.5 wt % Mg alloy as-quenched from 350° C.

prior to water quenching. Two types of grain-boundary enrichment were seen: a large scale enrichment such as shown in Fig. 5, and a significantly different profile shown in Fig. 6.

4. Discussion

Preliminary work identified depletion in 8 out of 11 boundaries tested in Al–6.5 wt % Mg alloys quenched from 350° C. This indicated that segregation/depletion could be detected in this alloy, and thus an attempt was made to characterize as-quenched solute profiles.

The profiles obtained from STEM work on the quenched Al–Mg alloys can be broken into four groups. The first group, Fig. 2, show depletion and this was observed only in alloys quenched from 350° C. Samples quenched from 350° C were aged at room temperature for 12 h. The second group, Figs 3 and 4, show enrichment on a fairly small scale. This type of profile was usually seen when the alloy was quenched from 400° C. The third group, Fig. 5, showed dramatic enrichment which occurred only when quenching from 570° C. The fourth group, Fig. 6, show enrichment both at the boundary and in the matrix on either side of the boundary to approximately 200 nm away. This type of profile was seen only in samples quenched from 570° C.

The most likely mechanism for grain-boundary depletion as seen in Fig. 2 is explained by rapid grain-boundary diffusion and the formation of precipitate plates at sites of easy nucleation on the grain-boundary when the alloy is quenched below 350° C into the two-phase region. The Al–Mg phase diagram shows that below about 300° C, second-phase precipitates of Mg_2Al_3 are stable in this alloy composition. It is likely that the grain-boundary region provides sites which allow precipitates to begin to form as pre-precipitate nuclei during or immediately after the quench. Grain boundaries provide a fast diffusion path which allows magnesium atoms on the boundary to migrate to nucleation sites both during and after the quench. As the precipitate nuclei grow somewhere in the boundary, the boundary itself is being depleted. This explanation, however, would predict the presence of precipitates on the grain boundary. While none were observed, no special effort was made to observe them using the TEM. STEM observation of very small, thin particles on the boundary was also unlikely due to the low contrast characteristics of the STEM. In addition, samples quenched from 350° C were not stored in liquid nitrogen, thus depletion on the grain-boundary could also have occurred as the nuclei coarsened at room temperature. The observation that three of the eleven boundaries, tested initially by comparing boundary composition

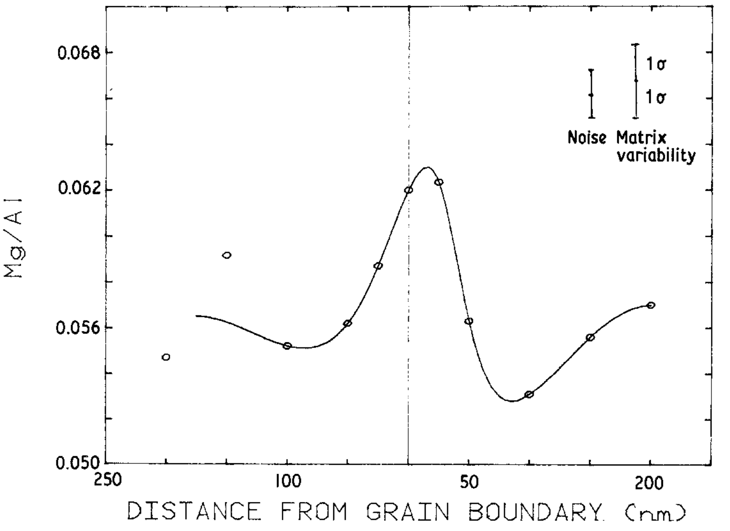

Figure 3 EDX analysis showing the solute concentration profile of a grain boundary in an Al–6.5 wt % Mg alloy as-quenched from 400° C and aged at room temperature for 18 h.

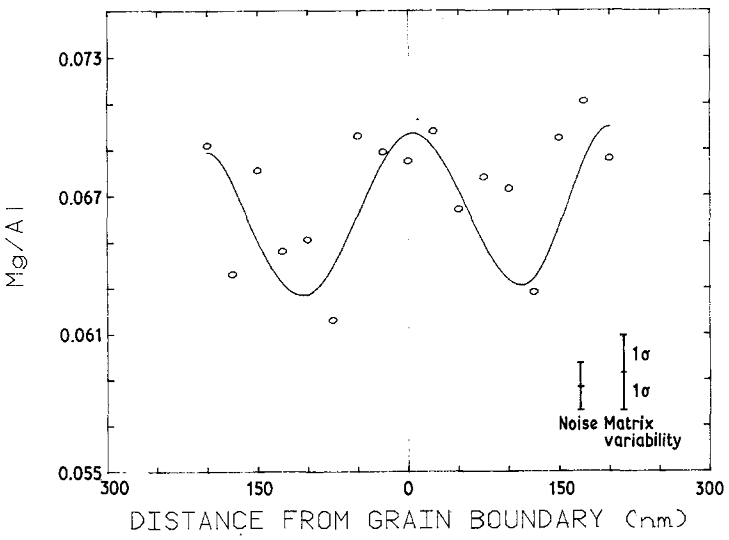

Figure 4 EDX analysis showing the solute concentration profile of a grain boundary in an Al–6.5 wt % Mg alloy as-quenched from 400° C.

to matrix composition, showed significant enrichment (Table I) may suggest that local precipitate nuclei were inadvertently analysed in these cases.

Depletion of grain boundaries in samples from 350° C is described in terms of precipitation and growth of nuclei which consequently deplete the boundary region. In a similar manner the profiles which resulted from quenching the alloy from 570° C can be described by a non-equilibrium segregation and precipitation mechanism.

The large enrichments shown in Fig. 5 can only be explained by non-equilibrium segregation by vacancy drag. It is predicted by non-equilibrium segregation theory (e.g. [7]) that increasing quench temperature leads to increasing solute enrichment in the grain-boundary region. This is clearly the case in Fig. 5, where enrichment is a factor of two to four greater than in any of the 400° C quenched alloy grain boundaries (e.g. Figs 3 and 4). This large enrichment should, if sites of easy nucleation are present, lead to precipitation which would subsequently consume the portion of the solute enrichment which is centred around the boundary. This would lead to the profiles seen in Fig. 6, where the central peaks are a result of thin precipitates regularly spaced in the boundary, while the secondary peaks in the matrix are the areas of non-equilibrium solute enrichment unaffected by the precipitation process as the boundary regions become depleted.

The profiles showing large enrichment (Fig. 5) can be understood by considering the types of boundaries which, while they are good vacancy sinks, do not possess sites of easy nucleation. The efficiency of a boundary as a point-defect source or sink has been shown to vary considerably [8]. Low-energy boundaries, for example, have been shown to be less efficient than random high-angle boundaries. The idea that all grain-boundaries are heterogeneous nucleation sites has been shown by Gronsky and Furrer [9] to be untenable in Al–Mg–Zn and Al–Zn alloys. Grain-boundaries whose structure does not provide many nucleation sites, but which are still operative as vacancy sinks, will undergo some enrichment but will not suffer the depletion of solute associated with grain-boundary precipitation.

The present result can be reconciled with previously published studies. In the present work, the presence of precipitates or pre-precipitation nuclei was not uniquely established. However, considerable evidence in the literature suggests the presence of these structures. Unwin *et al.* [10], for example, found considerable indirect evidence of precipitable nuclei at grain boundaries in the Al–Mg system. Further, the work of Cundy *et al.* [4], using EELS analyses, shows composition

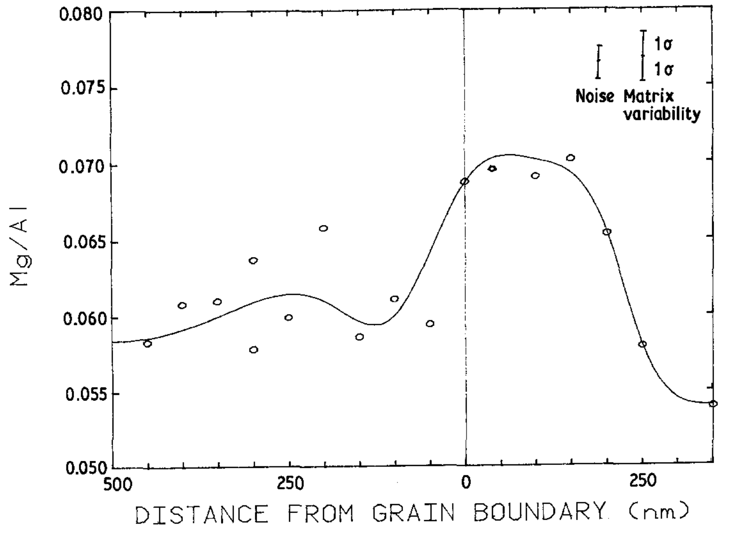

Figure 5 EDX analysis showing the solute concentration profile of a grain boundary in an Al–6.5 wt % Mg alloy as-quenched from 570° C. A large, widespread, enrichment of solute at the boundary can be seen. The slightly offset central magnesium concentration peak may be due to preferential electron channelling effects in one of the grains.

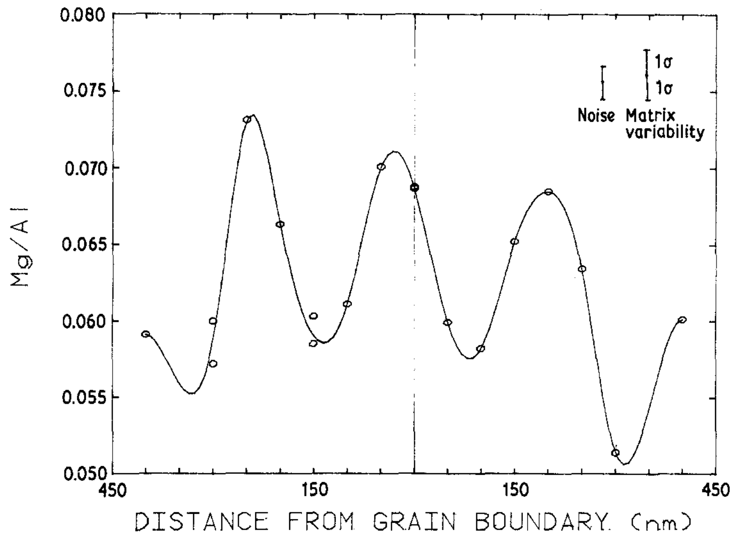

Figure 6 EDX analysis showing solute concentration profile of a grain boundary in an Al–6.5 wt % Mg alloy as-quenched from 570° C. A central peak on the grain boundary and enriched shoulders in the matrix can be seen.

profiles of grain-boundaries in Al–8 wt % Mg quenched from 350 and 540° C which are very similar to the present results. Cundy *et al.*, however, observed depletion at both quench temperatures. At the higher quench temperature (540° C) solute-enriched zones about 75 to 100 nm from the boundary were seen in the grains adjacent to the depleted boundary. These enriched zones, seen using EELS, correspond to the peaks seen in the present work in Fig. 6. At the lower quench temperature (350° C) a sharp peak slightly offset (10 nm) from the boundary was seen to be located within a much wider (150 nm) depleted zone. The profile of the depleted zone (ignoring the central peak) is similar to that seen in Figs 3 and 4. By superimposing these two EELS results, it appears that a profile similar to that seen in Fig. 6 would be obtained. It is important to note that although Cundy *et al.* [4] proposed precipitation during the quench to explain both depletion and central grain-boundary enrichment, no precipitates were observed unless the material was given a short ageing treatment. After the ageing treatment, a fine dispersion of particles were clearly resolved on the boundary.

The above EELS results are important since more recent studies, using EDX, were limited to a minimum electron probe size of 20 nm and significantly lower beam currents. This leads to a significant loss in spatial compositional resolution. The present work, by virtue of the use of a dedicated STEM, allowed the use of a 1 nm probe size. This probe size is comparable to that used in the EELS work.

5. Summary

1. An Al–6.5 wt % Mg alloy, when water-quenched from 350° C, showed significant magnesium depletion at 8 out of 11 grain-boundaries tested by STEM-EDX microanalysis.
2. Solute profiles normal to grain-boundaries in an Al–6.5 wt % Mg alloy quenched from 400° C show degrees of enrichment which vary between negligible to small but statistically significant. The grain-boundary enrichment may be due to the presence of precipitate nuclei on the boundary.
3. Solute profiles normal to grain-boundaries in an Al–6.5 wt % Mg alloy quenched from 570° C show, in many cases, a narrow enriched zone at the boundary and, to approximately 150 nm in the matrix on either side of the boundary, regions of significant enrichment. These enriched regions can be attributed to non-equilibrium segregation by vacancy drag and the subsequent formation of grain-boundary precipitates which cause local depletion of the enriched zone. The central peak probably represents an array of thin unresolved precipitates or nuclei at the boundary itself, while the outer enriched zones are what remains of the non-equilibrium enrichment after precipitation.
4. Two Al–6.5 wt % Mg grain-boundary solute profiles showed large enrichment extending as far as 100 nm from the boundary. This is believed to be due to non-equilibrium segregation by vacancy drag, occurring to a boundary where precipitation has not taken place.

Acknowledgements

The authors thank Dr U. Erb for many helpful discussions and the Natural Sciences and Engineering Research Council of Canada for financial support.

References

1. G. M. SCAMANS and A. S. REHAL, *J. Mater. Sci.* **14** (1979) 2459.
2. P. DOIG, J. W. EDINGHAM and M. H. JACOBS, *Phil. Mag.* **31** (2) (1975) 285.
3. C. R. SHASTRY and G. JUDD, *Met. Trans.* **3** (1972) 779.
4. S. L. CUNDY, A. J. B. METHERELL, P. N. T. UNWIN and R. B. NICHOLSON, *Proc. R. Soc.* **A307** (1968) 267.
5. T. MALIS and M. C. CHATURVEDI, *J. Mater. Sci.* **17** (1982) 1479.
6. R. TIXIER, and J. PHILIBERT, in Proceedings of 5th International Congress on X-ray Microanalysis, edited by G. Mollenstedt and K. H. Gunkler (Springer-Verlag, Berlin, 1969) p. 180.
7. K. T. AUST, P. NIESSEN, R. E. HANNEMAN and J. H. WESTBROOK, *Acta Metall.* **16** (1968) 291.
8. H. GLEITER, *ibid.* **27** (1979) 187.
9. R. GRONSKY and P. FURRER, *Met. Trans.* **12A** (1981) 121.
10. P. N. T. UNWIN and R. B. NICHOLSON, *Acta Metall.* **17** (1969) 1379.

Received 15 January
and accepted 13 March 1986